

Received July 16, 2020, accepted July 25, 2020, date of publication July 30, 2020, date of current version August 11, 2020.

Digital Object Identifier 10.1109/ACCESS.2020.3013029

Pathological Gait Classification Using Kinect v2 and Gated Recurrent Neural Networks

KOOKSUNG JUN¹, YONGWOO LEE¹, SANGHYUB LEE¹, DEOK-WON LEE¹,
AND MUN SANG KIM¹, (Member, IEEE)

School of Integrated Technology, Gwangju Institute of Science and Technology, Gwangju 61005, South Korea

Corresponding author: Mun Sang Kim (munsang@gist.ac.kr)

This work was supported in part by the Ministry of Trade, Industry and Energy, South Korea, under Grant 10063300 and Grant 20003762, and in part by the Gwangju Institute of Science and Technology.

ABSTRACT With the development of depth sensors and skeleton tracking algorithms, many skeleton-based pathological gait classification methods have recently been proposed. However, these methods classify only simple gait patterns, and there is no approach to classify complicated gait patterns. In this paper, we classify 1 normal and 5 pathological gaits (antalgic, stiff-legged, lurching, steppage, and Trendelenburg gaits) by using a gated recurrent unit (GRU)-based classifier and 3D skeleton data. We collected skeleton datasets for 1 normal and 5 pathological gaits by using a multiperspective Kinect system. We developed the GRU classifier to classify the pathological gaits and compared its performance with that of other machine learning-based classifiers. Furthermore, we considered various joint groups to identify important and irrelevant joints for pathological gait classification and to improve the performance of the GRU classifier. When all skeleton data are used, the GRU classifier achieves a classification accuracy of 90.13%. A long short-term memory (LSTM)-based classifier achieves the next highest accuracy of 87.25%. The classification accuracy of the GRU classifier depends on the joint groups considered, and the classification accuracy increases to 93.67% when only leg joints are considered. This study indicates that various pathological gaits can be classified by using skeleton data and the GRU classifier. The proposed method can be used to support medical and clinical decisions. Furthermore, the results for various joint groups can be used to develop other methods in cases where only specific joint data are available because of environmental limitations.

INDEX TERMS Pathological gait classification, skeleton-based classification, gated recurrent unit, deep learning, kinect.

I. INTRODUCTION

Gait patterns are an important type of bioinformation used to support medical and clinical decisions [1]–[4]. These patterns are influenced by various factors, such as the physical characteristics and health of an individual. Weakness in or damage to some body parts can cause abnormal gait patterns, and the patterns can vary depending on the weakened body part. In other words, classifying abnormal gait patterns can help to identify weakened body parts and determine what disease or health issue may be affecting an individual.

As various depth sensors and skeleton recognition techniques have been developed, many methods for skeleton-based abnormal gait recognition have been proposed [5]–[19]. However, most of these methods focused

on determining whether a gait is normal or abnormal [5], [8]–[14], [19], whereas only a few studies focused on pathologically classifying gaits [6], [7], [16]–[18]. Furthermore, the target datasets were composed of only simple abnormal gaits, such as the dragging-foot gait and stiff knee gait [6], [16]. To improve skeleton-based pathological gait classification, it is necessary to classify more complex pathological gaits. In this paper, we classify 1 normal and 5 pathological gaits (the antalgic, stiff-legged, lurching, steppage, and Trendelenburg gaits) by using Kinect v2 and a gated recurrent unit (GRU) [20]. Skeleton data of the gaits to classify are shown in Fig. 1, and the details of the pathological gaits are given in Table 1.

Many methods that use machine learning for skeleton-based abnormal gait recognition have been proposed. Bayesian classifiers [13] and artificial neural network classifiers [14] were applied to skeleton data and gait

The associate editor coordinating the review of this manuscript and approving it for publication was Wenbing Zhao¹.

TABLE 1. Description of 5 pathological gaits to classify.

Pathological Gait	Characteristics	Causes
Antalgic Gait	Attempt to keep weight off the injured leg to avoid pain, shortening the stance phase of the injured leg	Pain in the foot, ankle, knee, or hip
Stiff-legged Gait	Stiffness of the problematic leg while walking, making an outward semicircle while swinging the problematic leg	Joint-related pathologies, such as rheumatoid arthritis
Lurching Gait	Lurching the trunk backward at the heel strike of the problematic leg to compensate for weakness of hip extension	Weakness or paralysis of the gluteus maximus muscle
Steppage Gait	Dorsiflexion problem in the problematic leg, lifting the problematic leg higher than normal to keep the toes from scraping the ground	Weakness or paralysis of the anterior tibialis muscle
Trendelenburg Gait	Moving the problematic hip up and the opposite hip down during the stance phase to balance the hip level, lurching the trunk toward the problematic side	Weakness or paralysis of the gluteus medius and gluteus minimus

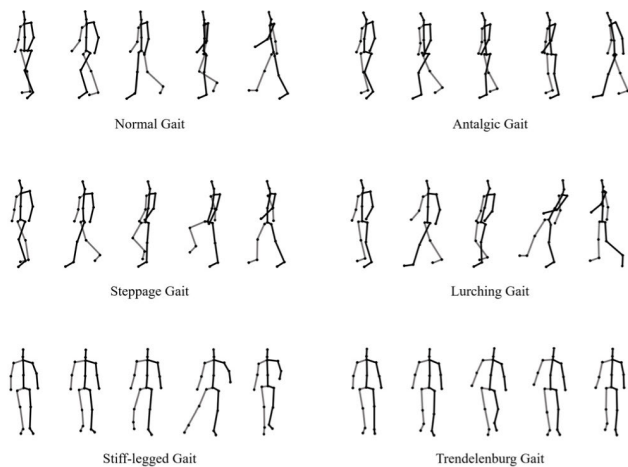


FIGURE 1. Skeleton data of normal and pathological gaits to classify.

features extracted from skeleton data, respectively, to identify Parkinson’s disease. Nguyen *et al.* [9] proposed a method for recognizing abnormal gaits using a hidden Markov model (HMM). Li *et al.* [7] extracted a covariance matrix from skeleton data and fed the matrix to a k-nearest neighbor (k-NN) classifier to identify abnormal gaits. Khokhlova *et al.* [6] identified abnormal gaits by using a long short-term memory (LSTM)-based ensemble model and the dynamic features of the lower limbs obtained from skeleton data. Jun *et al.* [16] extracted features from skeleton data by using a recurrent neural network (RNN)-based autoencoder and fed the features to classifiers to recognize abnormal gaits. Pachón-Suescún *et al.* [17] classified Parkinsonian, hemiplegic, and spastic diplegic gaits by using an LSTM. The datasets of the pathological gaits were generated by simulation of healthy people. They fed the sequence of distances from the hip center joint to each joint into the LSTM classifier. Chakraborty *et al.* [19] compared a logistic

regression model, a support vector machine, and multiple adaptive regression splines for detecting an equinus foot deformity gait. They used feature vectors constructed from angles of the hip, knee, and ankle of both sides as input data. In the data collection, healthy young subjects were asked to mimic an equinus foot deformity gait. Loureiro and Correia [18] used a skeleton energy image to classify normal, diplegic, and hemiplegic gaits simulated by healthy people. They used VGG-19 architecture to directly classify pathological gaits or to extract features from the skeleton energy image and fed them into linear discriminant analysis model or support vector machine for the classification.

In this paper, we propose a GRU-based classifier to classify pathological gaits. The GRU has a recurrent neural network (RNN) architecture that has a powerful processing ability for sequential data. Skeleton data are sequential data in a time series and there have been several approaches applying GRU to skeleton data [21]–[23]. Therefore, it is appropriate to apply GRUs for skeleton-based pathological gait classification. It is known that a GRU shows similar performance to an LSTM with fewer learning parameters. The GRU has been compared with an LSTM and has outperformed it in several classification studies [24]–[27]. We supposed that a GRU might outperform an LSTM in pathological gait classification and compared the performance of both models to verify the hypothesis.

In this paper, we attempted to classify 5 complicated pathological gait patterns for the first time. Most of the previous gait classification methods only considered simple abnormal gait patterns that could be easily classified. However, to support a physician’s decision, it is better to classify various gait patterns and identify a weakened body part specifically rather than solely determine whether the gait is normal or not. Furthermore, we fed data for various joint groups to the GRU classifier to identify the important and irrelevant joints for pathological gait classification.

The irrelevant joints decrease the classification performance, so it is important to select the necessary joints for classification. There have been a few approaches to classify gait patterns by using different joint groups [28]–[31]. However, the number of joint groups was not sufficient to clarify the influence of each joint. Alternatively, some works used various features, such as joint angles, which could also not clearly explain the relationship between joints and the effect of their combination in pathological gait classification. In this paper, we constructed 20 joint groups by using or excluding specific joints and tested the classification performance. We improved the classification performance by selecting the specific joints and clarified the important and unnecessary joints for the classification. Furthermore, the classification performances of all joint groups support the feasibility of utilizing specific joints for gait classification in limited environments.

The contributions of this paper are as follows:

- We share the skeleton datasets of the pathological gaits with the public. The datasets contain the antalgic, stiff-legged, lurching, steppage, and Trendelenburg gaits of 10 people (10 people \times 6 gait types \times 120 instances). The datasets are larger and more varied than other skeleton datasets of simulated abnormal gaits.
- We classify various complicated pathological gaits with a greater than 93% classification accuracy by using the GRU classifier. The classification of pathological gaits can aid in identifying weakened body parts and determining the related cause.
- The proposed method can support medical and clinical decision-making by physicians. Furthermore, we show the potential to classify other gait patterns when their skeleton data are collected and trained by the model.
- We feed data for various joint groups to the GRU classifier and analyze the results. The performance of the GRU classifier is improved by removing the irrelevant joints and focusing on the important joints. The results can aid in the design of other pathological gait classification schemes.

This paper is an extended version of a preliminary conference report that we presented at the 41st International Conference of the IEEE Engineering in Medicine and Biology Society (EMBC), Berlin, Germany, 2019 [15]. In the previous work, an LSTM-based classifier was used to classify the same pathological gaits, and different joint groups were fed to the classifier. The same data collection system was used in our previous work. We conducted experiments by using only an LSTM classifier and did not compare it with other classifiers. Only 4 subjects participated in data collection, so it was hard to apply a cross-validation method in our previous work. We solely used a quarter of the datasets of each subject as test datasets. Consequently, the overall test accuracies were high, but the results were not very convincing. In this paper, 10 subjects participated in the data collection, and we applied leave-one-subject-out cross-validation in all experiments,

which could further improve the reliability of the evaluation results. Furthermore, we analyzed the accuracy, sensitivity, specificity and precision for a single gait type, whereas our previous work considered only the test accuracy. In this paper, we also increased the diversity of the joint groups to achieve more systematic results. We compared classification performances of various classifiers, whereas only the LSTM classifier was used in our previous work. In addition, the GRU classifier proposed in this paper was shown to achieve a better performance than the LSTM classifier of our previous work.

II. METHODS

A. DATA COLLECTION

We collected skeletal gait data by using Kinect v2. Specifically, 3D coordinates of 25 joints were obtainable by using Kinect v2 and Microsoft SDK. We developed a multiperspective Kinect system using 6 sensors and calibrated each sensor. If the sensors were not calibrated, their coordinate systems would differ. It was necessary to calibrate the sensors to obtain direction-consistent data. We used a fiducial marker called ArUco [32] and Microsoft SDK to calibrate each sensor, as shown in Fig. 2. The left-bottom corner of the ArUco marker was set as an origin, and the directions of x and y are set as vectors from the origin toward the right side and toward the upside, respectively. The z-direction was determined by the cross-product of the x-direction and y-direction. We transformed the xyz-coordinate system of Kinect to the xyz-coordinate system of ArUco marker by applying a rotation and translation matrix. Three ArUco markers were attached to the ground, and sensors on the same line were calibrated to the xyz-coordinate system of the same ArUco marker, as shown in Fig. 2. Thus, the calibrated sensors had the same xyz-directions, so they collected consistent data from different positions.

We used Microsoft SDK to obtain skeleton data from Kinect. Skeletons were generated by each sensor individually. Therefore, 6 different skeleton data points were obtained when a walker passed through the walkway. Each sensor requires a single PC to use Microsoft SDK. We installed 6 Intel NUC PCs to use 6 Kinect sensors and 1 desktop PC to control the sensors. When a user enters the user name and clicks a start button, the desktop PC sends a signal to each NUC PC by using the TCP/IP network. Then, each NUC PC starts to collect skeleton data and stops the collection when the distance between the user and the sensor is less than 1 m. If the NUC PCs on the last line stop the data collection, they send a signal to notify the end of the data collection.

Ten healthy people participated in the data collection process and were asked to simulate antalgic, stiff-legged, lurching, steppage, and Trendelenburg gaits. The 5 pathological gaits to classify are relatively easily simulated compared to other pathological gaits because they can be simulated by limiting physical functions, such as joint rotation and flexion, in a mechanical way. If the cause of pathological

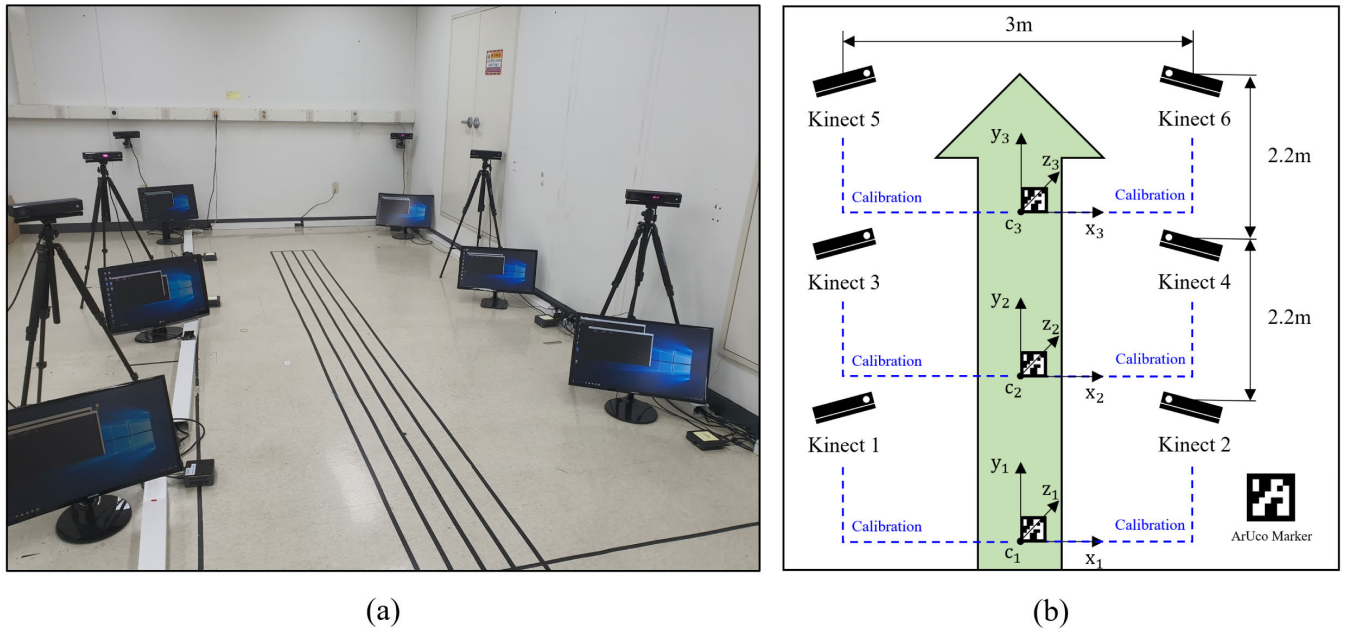


FIGURE 2. Gait data collection system. (a) View of the setup. (b) System specifications.

gait is related to the sensory or cognitive system, it is difficult to simulate the gait naturally and takes a long time to train a subject. We prepared guidelines for simulating the 5 pathological gaits and collected the datasets after the subject became familiar with simulating them. The guidelines for simulating the 5 pathological gaits were as follows:

- When simulating antalgic gait, keep the weight off one leg and minimize the time during which that leg touches the ground.
- When simulating stiff-legged gait, do not bend the knee of one leg and make an outward semicircle when swinging that leg.
- When simulating lurching gait, lurch the trunk backward upon heel strike of one leg.
- When simulating steppage gait, scrape the ground with the toe of one leg and lift the knee of that leg higher than normal.
- When simulating Trendelenburg gait, raise the hip of one leg and lurch the trunk toward the side of the leg when the foot of the leg touches the ground.

Each person walked 20 times for each gait, so 10 people \times 6 gait types \times 120 instances were obtained. The datasets have been shared on GitHub (see https://github.com/kooksung/pathological_gait_datasets).

B. GRU CLASSIFIER

RNN models are effective neural networks for handling time series of data such as text, sounds, and human gestures [33]–[42]. Above all, GRUs have a powerful RNN architecture. In this paper, a multilayered GRU classifier is utilized for skeleton-based pathological gait classification.

In the GRU classifier, the input data are in time series form. The number of input data points varies by joint group, and the time sequence of the input data is fixed at 50 frames. In this paper, \mathbf{x}_t denotes the input from time frame t . Before \mathbf{x}_t is fed to the input layer of the GRU classifier, \mathbf{x}_t is activated by a rectified linear unit function (ReLU) [43]. The equation for the activated input \mathbf{a}_t is:

$$\mathbf{a}_t = \text{ReLU}(\mathbf{W}_{\mathbf{x}\mathbf{a}}\mathbf{x}_t + \mathbf{b}_{\mathbf{a}}) \tag{1}$$

where $\mathbf{W}_{\mathbf{x}\mathbf{a}}$ and $\mathbf{b}_{\mathbf{a}}$ denote the weights and biases of \mathbf{a}_t , respectively. The GRU has a reset gate and update gate in each unit. Since it simultaneously forgets and updates memory cells, the GRU can overcome the vanishing gradient problem of the basic RNN model [44], [45]. The reset gate \mathbf{r}_t and update gate \mathbf{z}_t are composed of equations with respect to the activated input \mathbf{a}_t and the previous hidden state \mathbf{h}_{t-1} as follows:

$$\mathbf{r}_t = \sigma(\mathbf{W}_{\mathbf{a}\mathbf{r}}\mathbf{a}_t + \mathbf{W}_{\mathbf{h}\mathbf{r}}\mathbf{h}_{t-1} + \mathbf{b}_{\mathbf{r}}) \tag{2}$$

$$\mathbf{z}_t = \sigma(\mathbf{W}_{\mathbf{a}\mathbf{z}}\mathbf{a}_t + \mathbf{W}_{\mathbf{h}\mathbf{z}}\mathbf{h}_{t-1} + \mathbf{b}_{\mathbf{z}}) \tag{3}$$

where \mathbf{W} and \mathbf{b} denote the weights and biases of each gate, respectively. These equations also include the sigmoid function σ , which converts all real values to values in a range from 0 to 1. The reset gate and update gate are defined by a similar form, but the corresponding calculations involve different weights and biases. The GRU uses the combination of these two gates to update the current hidden state \mathbf{h}_t as follows:

$$\mathbf{h}_t = (1 - \mathbf{z}_t) \circ \mathbf{h}_{t-1} + \mathbf{z}_t \circ \tanh(\mathbf{W}_{\mathbf{a}\mathbf{h}}\mathbf{a}_t + \mathbf{r}_t \circ \mathbf{W}_{\mathbf{h}\mathbf{h}}\mathbf{h}_{t-1} + \mathbf{b}_{\mathbf{h}}) \tag{4}$$

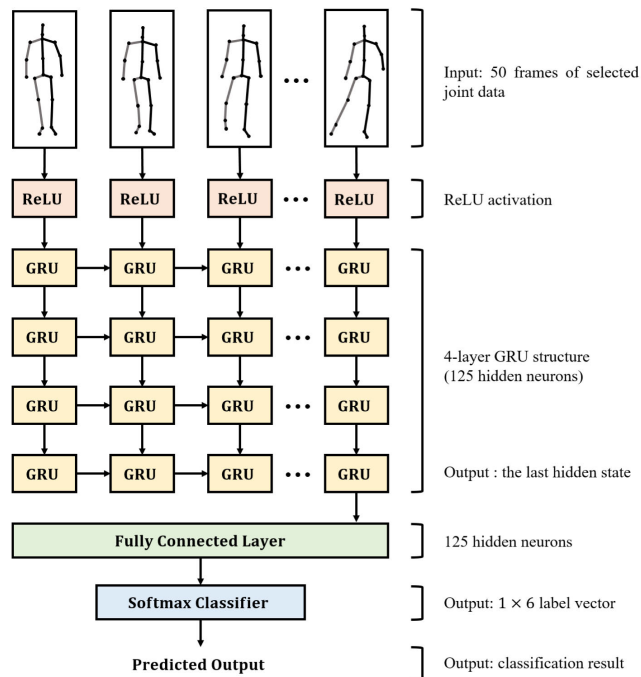


FIGURE 3. Structure of the GRU-based classifier.

where the operator \circ denotes the Hadamard product. Using the reset gate and update gate, hidden states are updated to distinguish and recognize necessary memory for classification. In the final frame, the last hidden state is determined, and this hidden state is fed to a fully connected layer to classify the data with the proposed GRU classifier. The final output $\hat{\mathbf{y}}$ indicates the (1×6) vector of the predicted result and is determined by the following equation:

$$\hat{\mathbf{y}} = \text{softmax}(\mathbf{W}_{\mathbf{h}\mathbf{y}}\mathbf{h}_T + \mathbf{b}_{\mathbf{y}}) \quad (5)$$

where $\mathbf{W}_{\mathbf{h}\mathbf{y}}$ and $\mathbf{b}_{\mathbf{y}}$ denote the weights and biases of the fully connected layer, respectively. A softmax classifier is used to determine the pathological gait based on the output of matrix multiplication in the form of a probability. The predicted class is the argument of the maximum value in $\hat{\mathbf{y}}$. The proposed GRU classifier is composed of 4-layer GRU neural networks, and each network has 125 hidden neurons.

C. JOINT SELECTION

The skeleton data in Kinect v2 contain the 3d coordinates of 25 joints, as shown in Fig. 4(a). Some of the joints have a positive impact on pathological gait classification and can be used to distinguish among different gait types and improve the GRU classification process. Additionally, some irrelevant joints have a negative impact on pathological gait classification. These joints make it difficult to identify differences among gait types and decrease the performance of the classifier. Therefore, we hypothesized that the performance of the GRU classifier can be improved by excluding the irrelevant joints that have a negative impact

on pathological gait classification. To identify the irrelevant and important joints, we divided the skeleton data into sets for various joint groups and fed them to the GRU classifier.

All joints in the skeleton are roughly divided into those for lower limbs (legs) and upper limbs (arms), and then they are divided into specific joint groups: neck and head, shoulders, elbows, spine, hands, hips, knees, and feet, as shown in Fig. 4(b). After dividing the joints, we controlled the input data for the GRU classifier by excluding one of the joint groups or only considering one joint group. We then analyzed the effect of each joint group on pathological gait classification. The objectives of this approach are summarized as follows:

- We intend to improve the performance of the GRU classifier by excluding the irrelevant joints and focusing on the important joints.
- The results for various joint groups can be used to design other pathological gait classification studies in which data for some joints are not available.

D. MODEL TRAINING

The GRU classifier was trained to classify 1 normal and 5 pathological gaits by using skeletal gait data. The selected joints are used as the inputs for the classifier. A single dataset contains approximately 80~90 frames of skeleton data. We did not use the first 10 frames of the data because of noise. We used the next 50 frames of the data for classification. If the number of frames was less than 60, we did not use the dataset. Therefore, among 7200 datasets (10 people \times 6 gaits \times 120 instances), we used 7157 for training and testing the classifier. The training process required a minimum of 500 iterations to satisfactorily train the classifier.

During the training process, the cross-entropy cost function and L2 regularization methods are used to train the classifier and prevent overfitting as follows:

$$L(\mathbf{x}, \mathbf{y}) = - \sum_{i=1}^6 y_i \log(\text{softmax}(\hat{y}_i)) + \frac{\lambda}{2} \|\mathbf{W}\|^2 \quad (6)$$

where $L(\mathbf{x}, \mathbf{y})$, λ , and \mathbf{W} denote the cost with the input data \mathbf{x} and the true one-hot vector label \mathbf{y} , the regularization parameter, and the trainable weights, respectively. We trained the model by using various optimizers and compared the results to find the most effective optimizer. We used the training results when the highest test accuracy was achieved.

We calculated the classification accuracy by using the leave-one-subject-out cross-validation method. Among the datasets of 10 subjects, the datasets of 1 subject were used for testing, and the datasets of the remaining subjects were used for training. We performed 10 repetitions to test the dataset of every subject. Finally, we obtained the classification accuracy by calculating the average test accuracy. Furthermore, we counted the true positives (TP), false positives (FP), true

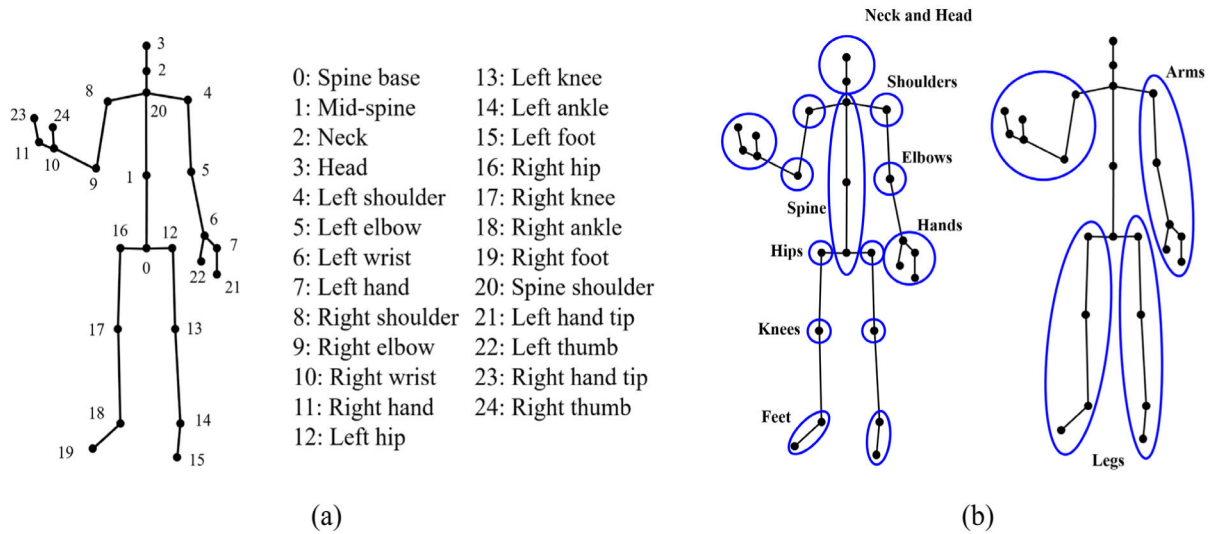


FIGURE 4. (a) Skeleton data from Kinect v2 and (b) grouped joints.

negatives (TN), and false negatives (FN) to calculate the accuracy, sensitivity, specificity and precision for a single gait type as follows:

$$\text{Accuracy} = \frac{TP + TN}{TP + FP + TN + FN} \quad (7)$$

$$\text{Sensitivity} = \frac{TP}{TP + FN} \quad (8)$$

$$\text{Specificity} = \frac{TN}{FP + TN} \quad (9)$$

$$\text{Precision} = \frac{TP}{TP + FP} \quad (10)$$

The configuration of the computer used for training consisted of an Intel® Core™ i7-7700K central processing unit (CPU), 16.00 GB random-access memory (RAM), and an NVIDIA GeForce RTX 2080-Ti. All classifiers used in this paper were developed by using TensorFlow.

III. RESULTS

We classified 1 normal and 5 pathological gaits by using the GRU classifier. To demonstrate the effectiveness of the GRU classifier, we also fed all the skeleton data into various machine learning-based classifiers and compared the results. In this experiment, we used the dataset of all joints as the input for the classifiers. We fed the skeleton data to the GRU classifier, an LSTM classifier, a basic RNN classifier, a convolutional neural network (CNN) classifier, a deep neural network (DNN) classifier, a k-nearest neighbor (k-NN) classifier, a k-means classifier, and a random forest classifier. For most of the neural network-based classifiers, such as the GRU, LSTM, basic RNN, and DNN classifier, a 4-layer structure and 125 hidden neurons on each layer were applied. Among them, the skeleton data were flattened and fed to the input layer for the DNN classifier. Only the CNN classifier had a different structure, where a 1D convolutional filter with

TABLE 2. Classification accuracy (%) of the models.

Model	Classification Accuracy
GRU	90.13
LSTM	87.25
RNN	86.23
CNN	86.65
DNN	85.86
k-NN	62.63
k-means	66.74
Random Forest	74.29

a filter size of 32 and 3 channels was attached to the input layer. The output of the convolutional filter entered fully connected layers that consisted of a 5-layer structure with 125 hidden neurons on each layer. Analogous to the DNN classifier, the flattened skeleton data were fed to the input layer in the CNN classifier.

Table 2 shows the classification accuracy of each classifier. The GRU classifier achieves the best performance with a 90.13% classification accuracy. The LSTM classifier ranks second with an 87.25% classification accuracy. The neural network-based classifiers performed better than the nonneural network-based classifiers, such as the k-NN, k-means, and random forest classifiers. With the configuration of the computer and training environment mentioned in Section II, it took 0.359 s, 0.355 s, 0.164 s, 0.072 s, and

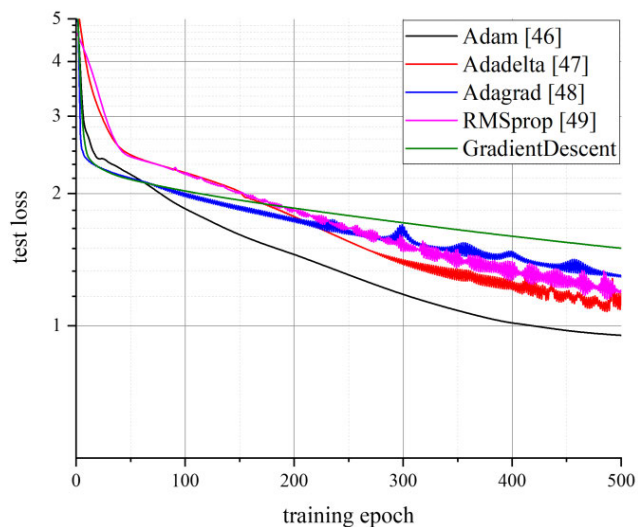


FIGURE 5. Loss curves of the GRU classifier for different optimizers.

0.312 s to train the GRU, LSTM, basic RNN, DNN, and CNN classifier, respectively, for a single epoch when feeding the data of all joints.

We trained the GRU classifier by using various optimizers (adaptive moment estimation (Adam) [46], adaptive learning rate method (Adadelta) [47], adaptive gradient method (Adagrad) [48], root mean square propagation (RMSprop) [49] and gradient descent) and compared the training results to determine the most effective optimizer. The loss curves for the optimizers are shown in Fig. 5. Among the optimizers, the Adam optimizer shows the best performance. The loss of the Adam optimizer converges at the fastest rate, which means the optimizer trains the GRU classifier more effectively than the other optimizers. We considered the Adam optimizer as the most appropriate optimizer to train the skeleton-based classification model composed of the GRU architecture. Therefore, we used Adam optimizer to train the GRU classifier in other experiments of this research.

To improve the performance of the GRU classifier, we controlled the input data fed to the classifier. We selectively fed certain joints by excluding or including specific joint groups and observed improvements in classification accuracy, as shown in Table 3. The results show that the performance of the GRU classifier depends on the joint group used as the input. As a control group, group A included all joints, and the classifier achieved a 90.13% classification accuracy. However, when only foot or leg joints are fed to the classifier (O9 and O10), the classification accuracy increases to 91.18% and 93.67%, respectively. Group O9 displays higher accuracy than group A even though only 4 joints out of a total of 25 were used. Group O10, which contains only leg joints, displays the best performance among all the groups. Furthermore, when excluding the leg joints, the classification accuracy decreases to 75.68%, which is the poorest performance among the E (joint selection by excluding specific joints) groups. These results show that the

leg joints are the most important joints for pathological gait classification.

Importantly, excluding the joints considered irrelevant to the classification task can increase the classification accuracy. As shown in Table 3, the performance is improved by excluding the elbows, hands or arm joints (E4, E5, and E6), which increases the classification accuracy to 90.45%, 91.25%, and 92.15%, respectively. These results show that the arm joints decrease the performance of the GRU classifier when all the joints are fed to the classifier.

The test loss curves of each group are shown in Fig. 6. The loss curve of group O10 converges to the lowest values at the fastest rate, which means the GRU-based classifier can more easily find a way to classify the pathological gaits when using only the legs. Group O7 (only hips) shows the highest loss value among all groups. The losses of all groups decrease at the early phase, but some of them start to increase at some training epoch. Thus, the model is overfitted to the training data and not generalized. Group O7 shows the largest increase. Although the hip joints are important in the pathological gait classification, they show their strength only if they are used with the joints of the knees and the feet. The losses of the O groups converge faster than those of the E groups. The number of input data is smaller in the O groups compared with the E groups. The smaller the number of input data, the earlier the training of the model finishes.

In this research, we achieved a 93.67% classification accuracy in pathological gait classification by using Kinect v2 and the GRU classifier. Furthermore, we also assessed the performance changes based on the various joint selections. In some cases, practically valid performance was achieved, even with limited joint data, and considering some joint groups even improved the performance compared to that obtained for the control group. These results support the feasibility of utilizing specific joints for gait classification in limited environments. For example, if the data of the hips are not collected accurately because of long and thick clothing, it is better to use only the feet joints (O9) than the joints except for the hips (E7).

IV. DISCUSSION

In this study, we confirmed that various pathological gaits can be classified using the skeleton data from Kinect v2 and the multilayered GRU classifier. Furthermore, we identified important and irrelevant joints for pathological gait classification by specifically considering various joint groups.

The GRU is an advanced RNN architecture that has displayed excellent performance comparable to LSTM classifiers. Since the GRU was introduced recently, it has not been verified that the GRU outperforms LSTM methods in all cases. However, these approaches have been compared in some research fields. In this paper, the GRU classifier exhibits better performance than the LSTM classifier, with a 2.88% higher classification accuracy, as shown in Table 2. This result indicates that the structure of the proposed GRU classifier is more appropriate and robust to overfitting than the LSTM

TABLE 3. Classification accuracy (%) and improvement (%) of the GRU classifier for different joint groups.

Annotation	Description	Selected Joints	Classification Accuracy	Improvement
A	All Joints	1,2,3,4,5,6,7,8,9,10,11,12,13,14,15,16,17,18,19,20,21,22,23,24	90.13	
E1	Joints except for spine	2,3,4,5,6,7,8,9,10,11,12,13,14,15,16,17,18,19,21,22,23,24	86.37	-3.76
E2	Joints except for neck and head	1,4,5,6,7,8,9,10,11,12,13,14,15,16,17,18,19,20,21,22,23,24	89.48	-0.65
E3	Joints except for shoulders	1,2,3,5,6,7,9,10,11,12,13,14,15,16,17,18,19,20,21,22,23,24	89.77	-0.36
E4	Joints except for elbows	1,2,3,4,6,7,8,10,11,12,13,14,15,16,17,18,19,20,21,22,23,24	90.45	+0.32
E5	Joints except for hands	1,2,3,4,5,8,9,12,13,14,15,16,17,18,19,20,21	91.25	+1.12
E6	Joints except for arms	1,2,3,12,13,14,15,16,17,18,19,20	92.15	+2.02
E7	Joints except for hips	1,2,3,4,5,6,7,8,9,10,11,13,14,15,17,18,19,20,21,22,23,24	89.23	-0.90
E8	Joints except for knees	1,2,3,4,5,6,7,8,9,10,11,12,14,15,16,18,19,20,21,22,23,24	87.64	-2.49
E9	Joints except for feet	1,2,3,4,5,6,7,8,9,10,11,12,13,16,17,20,21,22,23,24	82.45	-7.68
E10	Joints except for legs	1,2,3,4,5,6,7,8,9,10,11,20,21,22,23,24	75.68	-14.45
O1	Only spine	0,1,20	64.59	-25.54
O2	Only neck and head	2,3	55.74	-34.39
O3	Only shoulders	4,8	54.16	-35.97
O4	Only elbows	5,9	54.38	-35.75
O5	Only hands	6,7,10,11,21,22,23,24	65.39	-24.74
O6	Only arms	4,5,6,7,8,9,10,11,21,22,23,24	71.27	-18.86
O7	Only hips	12,16	48.29	-41.84
O8	Only knees	13,17	79.97	-10.16
O9	Only feet	14,15,18,19	91.18	+1.05
O10	Only legs	12,13,14,15,16,17,18,19	93.67	+3.54

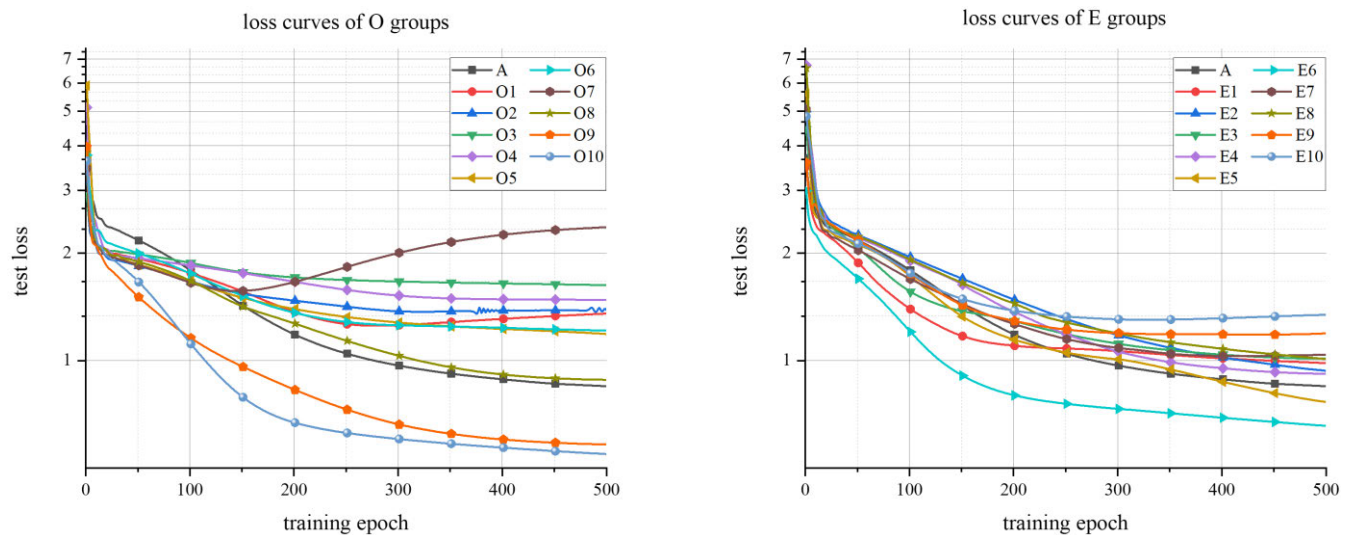


FIGURE 6. Loss curves of O groups and E groups.

classifier when classifying pathological gaits using skeleton-based gait data.

In neural networks, it is difficult to minimize the impact of irrelevant data while maximizing the amount of data used during training. Therefore, excluding irrelevant data before feeding the data to the GRU classifier can improve classifier performance. In this study, we divided the skeleton into various joint groups and fed them to the GRU classifier to verify the impact of each joint group on classification.

The results show that the spine, neck, and head joints are less influential than the other groups, as supported by the fact that the classification accuracy slightly varies when those groups are excluded from classification. The leg joints have the highest influence among all the joints, and the classification accuracy decreased by 14.45% when the leg joints were excluded. Since analyzing pathological gaits requires considering the weakness of an individual's lower limbs, it is reasonable to conclude that leg joints play a key

TABLE 4. Accuracy (%), Sensitivity (%), Specificity (%), and Precision (%) of group A (all the joints) and group O10 (only the legs).

Gait type	Group A (All joints)				Group O10 (Only legs)			
	Accuracy	Sensitivity	Specificity	Precision	Accuracy	Sensitivity	Specificity	Precision
Normal	96.67	98.70	96.28	83.66	97.79	98.88	97.58	88.75
Antalgic	96.65	83.83	99.23	95.63	98.64	94.67	99.45	97.18
Stiff legged	98.77	95.58	99.41	97.04	98.20	96.08	98.62	93.36
Lurching	95.01	86.92	96.64	83.91	96.81	87.50	98.69	93.09
Steppage	97.16	92.17	98.17	91.03	98.34	92.08	99.60	97.87
Trendelenburg	95.92	83.67	98.39	91.27	97.50	92.83	98.44	92.29

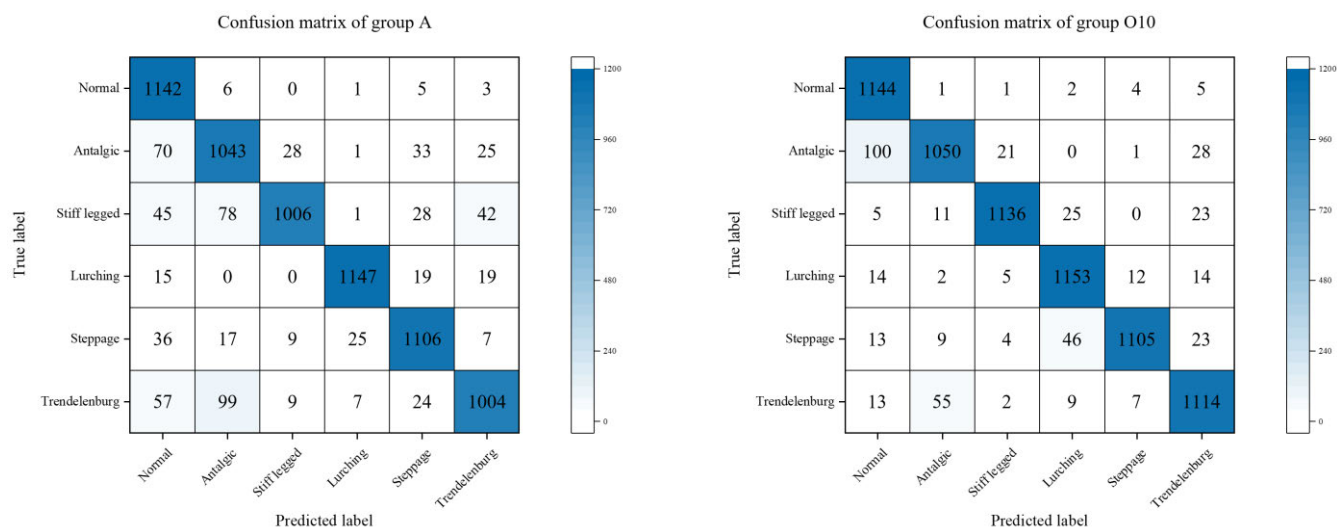


FIGURE 7. Confusion matrix of group A and group O10.

role in pathological gait classification. Conversely, arm joints have a negative impact on pathological gait classification. The subjects had different arm swing patterns when they walked, which influenced pathological gait classification. The inconsistent arm swing patterns of the subjects can confuse the classifier and decrease the performance of pathological gait classification. Therefore, the classification accuracy can be increased by excluding arm joints from the skeleton data fed to the classifier. However, it is still controversial to conclude that upper limbs do not play a critical role in pathological gait classification because some gait disorders have been diagnosed by reduced arm swings [50].

Considering only specific joint groups can help to effectively improve pathological gait classification systems in cases in which data for only some joints are available or accurate. For example, if knee data are not accurately collected because the walker is wearing a knee pad, it may be better to use only foot joints (O10) than to exclude the knee joints (E8). Moreover, if the view of the sensor is limited, the upper body joints should be excluded to focus on

accurately collecting the leg joint data instead. It is important to select joints depending on the environment, and the results in Table 3 can be used to design classification systems and improve their performance.

Table 4 shows the accuracy, sensitivity, specificity, and precision for each gait type when data for all joints (A) and only leg joints (O10) are fed into the model. The highest classification accuracy among all the groups is observed for group O10. The overall performance is improved when using only leg joints instead of all joints. In particular, the sensitivities of the antalgic and Trendelenburg gaits are increased by 10.84% and 9.16%, respectively, in this case. Thus, the GRU classifier more accurately classifies the antalgic and the Trendelenburg gaits when unimportant joint groups are excluded. Furthermore, the precisions of the lurching, steppage, and normal gaits are improved by 9.18%, 6.84%, and 5.09%, respectively, when unimportant joint groups are excluded. When all skeleton data are used, the GRU classifier is likely to misclassify input gait types as lurching, steppage, or normal gaits. Using only leg joint data allows the GRU classifier to avoid confusion. These

results suggest that using only leg joints can help the GRU classifier distinguish among the different pathological gaits and improve the classification performance.

The corresponding confusion matrices of group A and group O10 are shown in Fig. 7. The overall classification accuracy is higher in group O10. However, there are some issues to be considered. When feeding antalgic gait data, misclassification as normal gait is more likely in group O10 than in group A. On the other hand, antalgic gait is more frequently misclassified as steppage gait in group A than in group O10. For stiff-legged gait and steppage gait, group O10 shows much higher total accuracy than group A. However, both gaits are misclassified as lurching gait more frequently in group O10. The largest improvement is achieved in Trendelenburg gait. In group A, Trendelenburg gait is often misclassified as other gaits, especially normal gait or antalgic gait. On the other hand, in group O10, Trendelenburg gait is mostly correctly classified and is misclassified as antalgic gait less frequently than in group A.

V. CONCLUSION

In this paper, we propose a method to classify pathological gaits by using Kinect v2 and a GRU classifier. Furthermore, we feed the various joint groups to the classifier and analyze the results. We improve the performance of the GRU classifier by excluding the irrelevant joints and focusing on the important joints. The GRU classifier achieves a 93.67% classification accuracy by using only the leg joints. Furthermore, the performance of each joint group can be used to design other pathological gait classification studies in which usable joint data are limited. The proposed pathological gait classification method can help physicians make clinical decisions and contribute to improving smart home care systems. Since skeleton data can be easily collected in daily life without attaching any sensors, a gait classification system can be installed in the home and recommend that users visit a doctor if their gaits are classified as pathological gaits.

We confirmed that the various pathological gaits can be classified by using skeleton data and the GRU-based classifier if the datasets are collected and trained in a proper way. In future work, we plan to collect skeleton datasets of real patients by collaborating with hospitals and rehabilitation centers. We will also collect pathological gaits related to cognitive or sensory function that are difficult to simulate, such as Parkinsonian gait. Then, we will evaluate the GRU-based classifier by classifying these gait patterns.

REFERENCES

- [1] A. H. Snijders, B. P. van de Warrenburg, N. Giladi, and B. R. Bloem, "Neurological gait disorders in elderly people: Clinical approach and classification," *Lancet Neurol.*, vol. 6, no. 1, pp. 63–74, Jan. 2007.
- [2] T. A. L. Wren, G. E. Gorton, S. Öunpuu, and C. A. Tucker, "Efficacy of clinical gait analysis: A systematic review," *Gait Posture*, vol. 34, no. 2, pp. 149–153, Jun. 2011.
- [3] L. Brognara, P. Palumbo, B. Grimm, and L. Palmerini, "Assessing gait in Parkinson's disease using wearable motion sensors: A systematic review," *Diseases*, vol. 7, no. 1, p. 18, Feb. 2019.
- [4] R. A. Clark, B. F. Mentiplay, E. Hough, and Y. H. Pua, "Three-dimensional cameras and skeleton pose tracking for physical function assessment: A review of uses, validity, current developments and kinect alternatives," *Gait Posture*, vol. 68, pp. 193–200, Feb. 2019.
- [5] A. A. Chaaraoui, J. R. Padilla-Lopez, and F. Florez-Revelta, "Abnormal gait detection with RGB-D devices using joint motion history features," in *Proc. 11th IEEE Int. Conf. Workshops Autom. Face Gesture Recognit. (FG)*, May 2015, pp. 1–6.
- [6] M. Khokhlova, C. Migniot, A. Morozov, O. Sushkova, and A. Dipanda, "Normal and pathological gait classification LSTM model," *Artif. Intell. Med.*, vol. 94, pp. 54–66, Mar. 2019.
- [7] Q. Li, Y. Wang, A. Sharf, Y. Cao, C. Tu, B. Chen, and S. Yu, "Classification of gait anomalies from Kinect," *Vis. Comput.*, vol. 34, no. 2, pp. 229–241, Feb. 2018.
- [8] M. Meng, H. Drira, M. Daoudi, and J. Boonaert, "Detection of abnormal gait from skeleton data," in *Proc. 11th Joint Conf. Comput. Vis., Imag. Comput. Graph. Theory Appl.*, 2016, pp. 13–21. [Online]. Available: <https://hal.archives-ouvertes.fr/hal-01703237>
- [9] T.-N. Nguyen, H.-H. Huynh, and J. Meunier, "Skeleton-based abnormal gait detection," *Sensors*, vol. 16, no. 11, p. 1792, Oct. 2016.
- [10] T.-N. Nguyen, H.-H. Huynh, and J. Meunier, "Estimating skeleton-based gait abnormality index by sparse deep auto-encoder," in *Proc. IEEE 7th Int. Conf. Commun. Electron. (ICCE)*, Jul. 2018, pp. 311–315.
- [11] T.-N. Nguyen and J. Meunier, "Applying adversarial auto-encoder for estimating human walking gait abnormality index," *Pattern Anal. Appl.*, vol. 22, no. 4, pp. 1597–1608, Nov. 2019.
- [12] A. Paiement, L. Tao, M. Camplani, S. Hannuna, D. Damen, and M. Mirmehdi, "Online quality assessment of human motion from skeleton data," in *Proc. Brit. Mach. Vis. Conf.*, 2014, pp. 153–166.
- [13] A. Procházka, O. Vyšata, M. Vališ, O. Ťupa, M. Schätz, and V. Mařík, "Bayesian classification and analysis of gait disorders using image and depth sensors of microsoft kinect," *Digit. Signal Process.*, vol. 47, pp. 169–177, Dec. 2015.
- [14] O. Ťupa, A. Procházka, O. Vyšata, M. Schätz, J. Mareš, M. Vališ, and V. Mařík, "Motion tracking and gait feature estimation for recognising Parkinson's disease using MS kinect," *Biomed. Eng. OnLine*, vol. 14, no. 1, p. 97, Dec. 2015.
- [15] D.-W. Lee, K. Jun, S. Lee, J.-K. Ko, and M. S. Kim, "Abnormal gait recognition using 3D joint information of multiple kinects system and RNN-LSTM," in *Proc. 41st Annu. Int. Conf. IEEE Eng. Med. Biol. Soc. (EMBC)*, Jul. 2019, pp. 542–545.
- [16] K. Jun, D.-W. Lee, K. Lee, S. Lee, and M. S. Kim, "Feature extraction using an RNN autoencoder for skeleton-based abnormal gait recognition," *IEEE Access*, vol. 8, pp. 19196–19207, 2020.
- [17] C. G. Pachon-Suescun, J. O. Pinzon-Arenas, and R. Jimenez-Moreno, "Abnormal gait detection by means of LSTM," *Int. J. Electr. Comput. Eng. (IJECE)*, vol. 10, no. 2, p. 1495, Apr. 2020.
- [18] J. Loureiro and P. L. Correia, "Using a skeleton gait energy image for pathological gait classification," in *Proc. 15th IEEE Int. Conf. Auto. Face Gest. Recognit. (FG)(FG)*, May 2020, pp. 410–414.
- [19] S. Chakraborty, S. Jain, A. Nandy, and G. Venture, "Pathological gait detection based on multiple regression models using unobtrusive sensing technology," *J. Signal Process. Syst.*, pp. 1–10, Apr. 2020, doi: 10.1007/s11265-020-01534-1.
- [20] J. Chung, C. Gulcehre, K. Cho, and Y. Bengio, "Empirical evaluation of gated recurrent neural networks on sequence modeling," 2014, *arXiv:1412.3555*. [Online]. Available: <http://arxiv.org/abs/1412.3555>
- [21] S. Shin and W.-Y. Kim, "Skeleton-based dynamic hand gesture recognition using a part-based GRU-RNN for gesture-based interface," *IEEE Access*, vol. 8, pp. 50236–50243, 2020.
- [22] M. M. Islam, A. Lam, H. Fukuda, Y. Kobayashi, and Y. Kuno, "An intelligent shopping support robot: Understanding shopping behavior from 2D skeleton data using GRU network," *Robomech J.*, vol. 6, no. 1, p. 18, Dec. 2019.
- [23] S. Wei, Y. Song, and Y. Zhang, "Human skeleton tree recurrent neural network with joint relative motion feature for skeleton based action recognition," in *Proc. IEEE Int. Conf. Image Process. (ICIP)*, Sep. 2017, pp. 91–95.
- [24] R. Rana, "Gated recurrent unit (GRU) for emotion classification from noisy speech," 2016, *arXiv:1612.07778*. [Online]. Available: <http://arxiv.org/abs/1612.07778>
- [25] M. Zulqarnain, R. Ghazali, M. G. Ghouse, and M. F. Mushtaq, "Efficient processing of GRU based on word embedding for text classification," *JOIV, Int. J. Informat. Visualizat.*, vol. 3, no. 4, pp. 377–383, Nov. 2019.

- [26] H. M. Lynn, S. B. Pan, and P. Kim, "A deep bidirectional GRU network model for biometric electrocardiogram classification based on recurrent neural networks," *IEEE Access*, vol. 7, pp. 145395–145405, 2019.
- [27] H. Liu, H. Wu, W. Sun, and I. Lee, "Spatio-temporal GRU for trajectory classification," in *Proc. IEEE Int. Conf. Data Mining (ICDM)*, Nov. 2019, pp. 1228–1233.
- [28] P. Barra, C. Bisogni, M. Nappi, D. Freire-Obregon, and M. Castrillon-Santana, "Gender classification on 2D human skeleton," in *Proc. 3rd Int. Conf. Bio-Eng. Smart Technol. (BioSMART)*, Apr. 2019, pp. 1–4.
- [29] M. Ahmed, N. Al-Jawad, and A. T. Sabir, "Gait recognition based on Kinect sensor," *Proc. SPIE*, vol. 9139, May 2014, Art. no. 91390B.
- [30] E. Gianaria, N. Balossino, M. Grangetto, and M. Lucenteforte, "Gait characterization using dynamic skeleton acquisition," in *Proc. IEEE 15th Int. Workshop Multimedia Signal Process. (MMSP)*, Sep. 2013, pp. 440–445.
- [31] B. Dikovski, G. Madjarov, and D. Gjorgjević, "Evaluation of different feature sets for gait recognition using skeletal data from kinect," in *Proc. 37th Int. Conv. Inf. Commun. Technol., Electron. Microelectron. (MIPRO)*, May 2014, pp. 1304–1308.
- [32] S. Garrido-Jurado, R. Muñoz-Salinas, F. J. Madrid-Cuevas, and M. J. Marín-Jiménez, "Automatic generation and detection of highly reliable fiducial markers under occlusion," *Pattern Recognit.*, vol. 47, no. 6, pp. 2280–2292, Jun. 2014.
- [33] N. Ballas, L. Yao, C. Pal, and A. Courville, "Delving deeper into convolutional networks for learning video representations," 2015, *arXiv:1511.06432*. [Online]. Available: <http://arxiv.org/abs/1511.06432>
- [34] K. Cho, B. van Merriënboer, D. Bahdanau, and Y. Bengio, "On the properties of neural machine translation: Encoder-decoder approaches," 2014, *arXiv:1409.1259*. [Online]. Available: <http://arxiv.org/abs/1409.1259>
- [35] Y. Du, W. Wang, and L. Wang, "Hierarchical recurrent neural network for skeleton based action recognition," in *Proc. IEEE Conf. Comput. Vis. Pattern Recognit. (CVPR)*, Jun. 2015, pp. 1110–1118.
- [36] A. Graves, N. Jaitly, and A.-R. Mohamed, "Hybrid speech recognition with deep bidirectional LSTM," in *Proc. IEEE Workshop Autom. Speech Recognit. Understand.*, Dec. 2013, pp. 273–278.
- [37] A. Graves, A.-R. Mohamed, and G. Hinton, "Speech recognition with deep recurrent neural networks," in *Proc. IEEE Int. Conf. Acoust., Speech Signal Process.*, May 2013, pp. 6645–6649.
- [38] J. Liu, G. Wang, L.-Y. Duan, K. Abdiyeva, and A. C. Kot, "Skeleton-based human action recognition with global context-aware attention LSTM networks," *IEEE Trans. Image Process.*, vol. 27, no. 4, pp. 1586–1599, Apr. 2018.
- [39] M.-T. Luong, H. Pham, and C. D. Manning, "Effective approaches to attention-based neural machine translation," 2015, *arXiv:1508.04025*. [Online]. Available: <http://arxiv.org/abs/1508.04025>
- [40] N. Srivastava, E. Mansimov, and R. Salakhudinov, "Unsupervised learning of video representations using lstms," in *Proc. Int. Conf. Mach. Learn.*, Jun. 2015, pp. 843–852.
- [41] J. Yue-Hei Ng, M. Hausknecht, S. Vijayanarasimhan, O. Vinyals, R. Monga, and G. Toderici, "Beyond short snippets: Deep networks for video classification," in *Proc. IEEE Conf. Comput. Vis. Pattern Recognit. (CVPR)*, Jun. 2015, pp. 4694–4702.
- [42] W. Zhu, C. Lan, J. Xing, W. Zeng, Y. Li, L. Shen, and X. Xie, "Co-occurrence feature learning for skeleton based action recognition using regularized deep LSTM networks," in *Proc. AAAI Conf. Artif. Intell.*, 2016, pp. 3697–3703.
- [43] V. Nair and G. E. Hinton, "Rectified linear units improve restricted Boltzmann machines," in *Proc. 27th Int. Conf. Mach. Learn. (ICML)*, 2010, pp. 807–814.
- [44] R. Dey and F. M. Salem, "Gate-variants of gated recurrent unit (GRU) neural networks," in *Proc. IEEE 60th Int. Midwest Symp. Circuits Syst. (MWSCAS)*, Aug. 2017, pp. 1597–1600.
- [45] S. Hochreiter, "The vanishing gradient problem during learning recurrent neural nets and problem solutions," *Int. J. Uncertainty, Fuzziness Knowl.-Based Syst.*, vol. 06, no. 02, pp. 107–116, Apr. 1998.
- [46] D. P. Kingma and J. Ba, "Adam: A method for stochastic optimization," 2014, *arXiv:1412.6980*. [Online]. Available: <http://arxiv.org/abs/1412.6980>
- [47] M. D. Zeiler, "ADADELTA: An adaptive learning rate method," 2012, *arXiv:1212.5701*. [Online]. Available: <http://arxiv.org/abs/1212.5701>
- [48] J. Duchi, E. Hazan, and Y. Singer, "Adaptive subgradient methods for online learning and stochastic optimization," *J. Mach. Learn. Res.*, vol. 12, pp. 2121–2159, Feb. 2011.

- [49] T. Tieleman and G. Hinton, "Lecture 6.5-RMSProp: Divide the gradient by a running average of its recent magnitude," in *Proc. Coursera, Neural Netw. Mach. Learn.*, vol. 4, no. 2, pp. 26–31, 2012.
- [50] J. Jankovic, "Parkinson's disease: Clinical features and diagnosis," *J. Neurol., Neurosurg. Psychiatry*, vol. 79, no. 4, pp. 368–376, 2008.



KOOKSUNG JUN received the B.S. degree in mechanical engineering and the M.S. degree in intelligent robotics from the Gwangju Institute of Science and Technology, Gwangju, South Korea, in 2018 and 2019, respectively, where he is currently pursuing the Ph.D. degree. His current research interests include healthcare robotics, artificial intelligence, and pattern recognition.



YONGWOO LEE received the B.S. degree in mechanical engineering from the Gwangju Institute of Science and Technology, Gwangju, South Korea, in 2020, where he is currently pursuing the M.S. degree. His current research interests include smart healthcare systems, rehabilitation, artificial intelligence, and pattern recognition.



SANGHYUB LEE received the B.S. degree in biomedical engineering from the University of Ulsan, in 2017, and the M.S. degree in intelligent robotics from the Gwangju Institute of Science and Technology, in 2019, where he is currently pursuing the Ph.D. degree. His current research interests include image processing, healthcare robotics, and pattern recognition.



DEOK-WON LEE received the B.S. degree in electronics and electric wave and information engineering from Chungnam National University, in 2009, and the M.S. degree in electrical and electronics engineering from Yonsei University, in 2013. He is currently pursuing the Ph.D. degree with the Gwangju Institute of Science and Technology. His current research interests include healthcare robotics, artificial intelligence, and pattern recognition.



MUN SANG KIM (Member, IEEE) received the B.S. and M.S. degrees in mechanical engineering from Seoul National University, Seoul, South Korea, in 1980 and 1982, respectively, and the Dr.-Ing. degree in robotics from the Technical University of Berlin, Berlin, Germany, in 1987. From 1987 to 2016, he was a Research Scientist with the Korea Institute of Science and Technology, Seoul. He led the Advanced Robotics Research Center, in 2000. He was the Director of the Intelligent Robot—The Frontier 21 Program, in October 2003, which is one of the most challenging research programs, South Korea. He is currently a Professor with the School of Integrated Technology, Gwangju Institute of Science and Technology. His current research interests include healthcare robotics, UWB-based indoor localization systems, and culture technology.